

Nonlinear light propagation in cholesteric liquid crystals with a helical Bragg microstructure

Yikun Liu¹, Shenhe Fu¹, Xing Zhu¹, Xiangsheng Xie¹,
Mingneng Feng¹, Jianying Zhou^{1*}, Yongyao Li², Ying Xiang^{1,3},
Boris A. Malomed⁴, Gershon Kurizki⁵

¹State Key Laboratory of Optoelectronic Materials and Technologies, Sun Yat-Sen University,

Guangzhou 510275, China

²Department of Applied Physics, South China Agricultural University, Guangzhou 510642, China

³Information Engineering College, Guangdong University of Technology, Guangzhou, China

⁴Department of Physical Electronics, School of Electrical Engineering, Faculty of Engineering, Tel Aviv University, Tel Aviv 69978, Israel

⁵Chemical Physics Department, Weizmann Institute of Science, Rehovot 76100, Israel

E-mail: stszjy@mail.sysu.edu.cn

December 2014

Abstract. Nonlinear optical propagation in cholesteric liquid crystals (CLC) with a spatially periodic helical molecular structure is studied experimentally and modeled numerically. This periodic structure can be seen as a Bragg grating with a propagation stopband for circularly polarized light. The CLC nonlinearity can be strengthened by adding absorption dye, thus reducing the nonlinear intensity threshold and the necessary propagation length. As the input power increases, a blue shift of the stopband is induced by the self-defocusing nonlinearity, leading to a substantial enhancement of the transmission and spreading of the beam. With further increase of the input power, the self-defocusing nonlinearity saturates, and the beam propagates as in the linear-diffraction regime. A system of nonlinear couple-mode equations is used to describe the propagation of the beam. Numerical results agree well with the experiment findings, suggesting that modulation of intensity and spatial profile of the beam can be achieved simultaneously under low input intensities in a compact CLC-based micro-device.

1. Introduction

The propagation of light waves at frequencies near the propagation bandgap of nonlinear photonic structures is the subject of very broad interest [1, 2, 3, 4, 5, 6]. Most experiments in this field were performed in fiber Bragg gratings [7, 8], or other solid-state materials, which may be silicon-on-insulator and AlGaAs [9, 10]. Many applications rely on the use of nonlinear-optical effects, such as bistability [11], compression and shaping

of laser pulses [12, 13], generation of gap solitons [14, 15, 16], storage and buffering of ultrashort optical pulses [17, 18], ultrafast optical switches [19], etc.

In the spatial domain, Bragg solitons in continuous optical media were predicted in various settings, that can be implemented using planar waveguides and photonic crystals, but they have not yet been demonstrated experimentally. On the other hand, discrete gap solitons were created in arrays of waveguides with the self-focusing Kerr nonlinearity [20].

In this work, we study the nonlinear beam propagation in a dye-doped cholesteric liquid crystal (CLC), whose molecules are oriented so as to form a periodic helical order in the longitudinal direction [28], thus building a Bragg structure which affects circularly polarized light and creates a steep propagation stopband, with the spectral width close to 80 nm. An appropriate dopant added to the CLC matrix can reduce the nonlinear threshold by several orders of magnitude due to the additional dye torque [29, 30, 31, 32, 33, 34]. Thus, the strong nonlinearity gives rise to a low operational power, and requires shorter propagation lengths. These advantages provide simultaneous modulation of the beam's intensity and spatial structure at low input intensities in a compact sample.

We experimentally test the beam propagation in the CLC under different input powers. To this end, the light beam is selected with the carrier frequency located near the edge of the gap. A substantial increase of the transmission is observed with the increase of the input power, due to the blue shift of the propagation stopband induced by the self-defocusing nonlinearity. The output spot size is also measured, showing spreading of the beam under the action of the self-defocusing nonlinearity. With the further increase of the input power, the self-defocusing nonlinearity saturates, and finally leads to the propagation in the effectively linear-diffraction regime. Thus, CLC settings offer the advantage of implementing the simultaneous modulation to the beam's profile and intensity by a single compact device. To model the experimental setting, we use nonlinear couple-mode equations for the light propagation in the grating. The numerical results agree well with the experiment findings.

2. The cholesteric liquid crystals used in the experiment

The CLC medium, built of rod-like molecules, was produced by adding a chiral agent to nematic liquid crystal 5CB ($n_o = 1.53$, $n_e = 1.72$, $dn = 0.19$) supplied by Merck. The nematic phase exists in this material at temperatures from 18° C to 35° C, self-assembling to build a stacked periodic corkscrew-like structure, due to the helical twist introduced by the chiral agent. The average refractive index of the medium is 1.635, and its birefringence is 0.19. The pitch of the CLC structure can be controlled by the concentration of the chiral agent. Absorption dye is additionally doped into CLC to provide the dye torque and thus enhance the third-order nonlinearity.

The sample was fabricated with the thickness of 50 μm , and the density of the chiral agent was fixed at 17.4%, to induce the propagation stopband of the spectral width 80

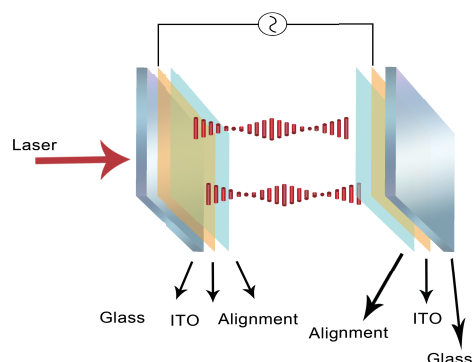


Figure 1. (Color online) A scheme of the setup.

nm, with the center set at 442 nm, and the red band edge at 468 nm. The CLC was doped by the DCM [4-(Dicyanomethylene)-2-methyl-6-(4-dimethylaminostyryl)-4*H*-pyran] laser dye with the absorption peak at 470 nm and the concentration of 1 wt%. Thus, suitable absorption can be achieved at the red edge of the stopband. The samples were sandwiched by two Indium Tin Oxide (ITO) glass substrates with a 50 μm thick spacer, coated by polyimide and rubbed unidirectionally to impose the planar alignment. The CLC sample was pulled into the cell by the capillary force. Molecules in the CLC are helically aligned in the same direction in the plane parallel to the cell surface. The scheme of the CLC sample is shown in Fig. 1.

Previous studies successfully analyzed photo-tunable characteristics of dye-doped CLCs [35, 36, 37]. Studies of nonlinear optical properties of CLCs in the direction perpendicular to the helix were reported before [38, 39]. The spatial properties of the nonlinear beam propagation were previously investigated in the direction perpendicular to the helix [40], which is determined by the spatial discrete diffraction (due to the coupling between the two adjacent waveguides) and nonlinear effect. In these previous work the linear and nonlinear properties of CLC were discussed, and nonlinear spatial propagation properties and spatial soliton was investigated in the direction perpendicular to the helix[41]. In the direction parallel to the helix, nonlinear effects have been already investigated[42, 43]. In this work, nonlinear spatial propagation in direction parallel to the helix will be investigated.

3. The experiment

The experimental setup for demonstrating the stopband shift is shown in Fig. 2(a). A xenon lamp was used as a white-light source with the circular light polarization to measure the reflection spectrum of the CLC. The pump is provided by an optical parametric oscillator operating at 468 nm, which is driven by a continuous mode-locked

Ti:sapphire femtosecond laser with repetition rate 80 MHz and pulse duration 100 fs. Here the femtosecond pulse is used for generating the nonlinearity. The pump field with wavelength at 468 nm is chosen for two reasons. First, the wavelength corresponds to the absorption peak of the dopant DCM, which gives rise to an additional dye torque acting on CLC molecules; second, such a wavelength is close to the red edge of the CLC stopband, which helps to observe a substantial increase of the transmission. The probe beam was shone normally to the CLC cell.

Another setup for measuring the beam-propagation profile is shown in Fig. 2(b). A single femtosecond probe beam was used for this purpose. The spatial evolution was evaluated by measuring the beam's waist after passing 50 μm in the sample before reaching a CCD detector, starting with a tightly focused input.

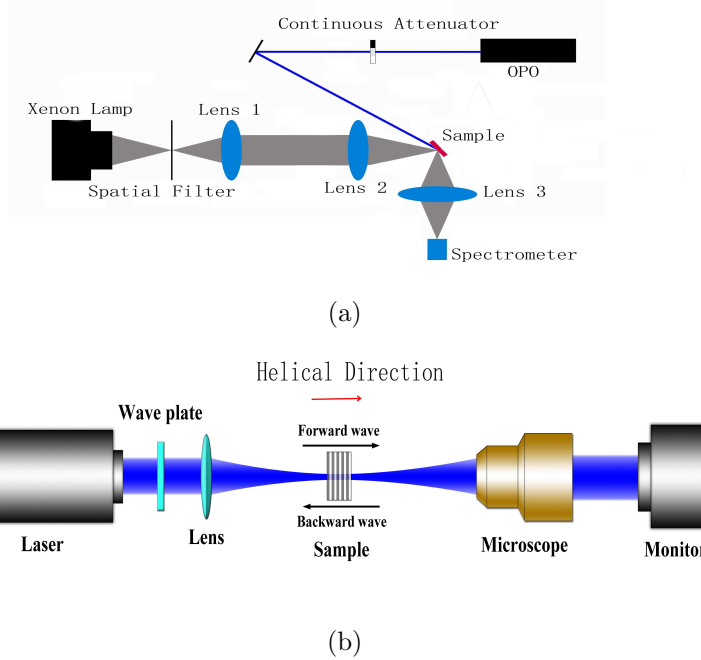


Figure 2. (Color online) Schematics of the experimental setups for measuring the reflection spectra under pumping (a), and the transmission profile (b). In the latter case, a single pump beam is used.

As mentioned above, in our experiment the width of the stopband is 80 nm, and its edge is steep enough to generate a substantial variation in the reflection/transmission due to a small shift of the stopband. At an average pump power of 85 mW (the corresponding peak-power density is 1.25 MW/cm^2), blue shift of the central wavelength of stopband is observed (Fig. 3). According to the Bragg formula, the central wavelength of the propagation stopband is $\lambda_B = 2n_{\text{eff}}d$, where d and n_{eff} are the structural period and average refractive index of the CLC. The bandwidth of the stopband, $\Delta\lambda$, is determined by $\Delta\lambda = 2dn \cdot d$, where dn is the refractive index modulation in the CLC. In the experiment, only the shift of the stopband center is observed, without a change

of the bandwidth. This result suggests that the change of the average refractive index is the main mechanism underlying the stopband shift.

The change of the refractive index in liquid crystals can be attributed to various causes, such as the ultrafast Kerr effect [44], the thermal [45] and photorefractive [46, 47] effects, and the dye torque [29]. According to Ref. [44], in an undoped CLC sample, optical intensity higher by a factor of 10^3 was needed to produce the same shift of the stopband as in the DCM-doped sample. This means the DCM dopant plays a crucially important role for the shift.

To examine the contribution of the thermal effect to the CLC nonlinearity, two additional experiments have been carried out. (1) A continuous-wave, non-mode-locked laser with the same average power as that of the mode-locked femtosecond laser, was applied to illuminate the sample. In this case, no nonlinear shift of the stopband was observed, thus demonstrating that an intensity-dependent nonlinear effect determines the shift, rather than the average power that would be related to a thermally-induced effect. (2) A pumping femtosecond pulse train with 2 kHz chopping, for which the thermal effect should be much lower than in the case of a continuous pulse, was also used to measure the stopband change. The result is compared to that without chopping, showing that the nonlinear shift of the bandgap does not depend on the chopper's rate. This observation further suggests that the thermal effect plays a negligible role in generating the nonlinear-optical effect. The result obtained with the continuous wave suggests that the photorefractive effect is not significant either for generating the stopband shift.

Thus, the optical torque is a plausible mechanism which underlies the nonlinear effect in the CLC. As a strong pulse is applied to the medium, an additional dye torque is generated, leading to rotation of the CLC molecules, and changing the refractive index. This outcome is not produced by thermo-optical effects [45] induced by laser heating. Instead, the dye torque is generated by electronically excited dye molecules, which is known as the *Janossy effect*. [29, 30, 31, 32, 33, 34].

The blue shift of the stopband indicates that the average refractive index is reduced by the high-intensity pump, which may be construed as a self-defocusing Kerr effect. In the initial situation without a pump pulse, the rod-like molecules are oriented perpendicular to the helix direction, which corresponds to the maximum refractive index. Under the action of the pump beam, the molecules rotate out of cell plane, which leads to a decreased refractive index. This means without the excitation of pumping light, the molecules orientate perpendicular to the helix and paralleled to the polarization of pumping light, which give the refractive index n_e . As the sample are pumped by femtosecond pulse, the pumping light excite the dye, the dye will exert a dye-torque to reorient the LC molecules with angle θ with respect to cell plane, which result in the effective diffractive index $n_{eff}(\theta)$, obviously, $n_{eff}(\theta) < n_e$. In the experiment, we always observed the blue shifting of the stop band, and never observe red shifting, this result confirm the conclusion of rotate of LC out of the plane. This dye-torque should be ascribed to the Jannossy effect, as ref. 42 indicated that for pure CLC the pumping

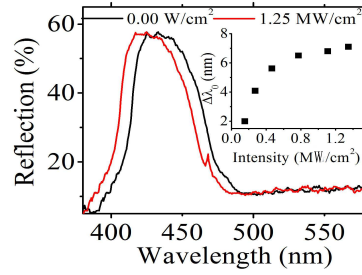


Figure 3. (Color online) The reflection spectra produced by the CLC sample. The photonic bandgap can be shifted under the action of the pump. The inset shows experimental data for the shift of the bandgap as a function of the pump power.

intensity should be about 1000 times higher. Due to the saturable absorption by the dopant dye, the additional dye torque saturates too, eventually leading to the saturation of the stopband shift. Accordingly, the inset in Fig. 3 shows that the shift increases with the increase of the pump power, and then reaches saturation when the pump power exceeds 0.7 MW/cm^2 .

An obvious difference from the fiber Bragg gratings is that the transverse field distribution in the CLC is not limited by the cross section of the fiber, hence various phenomena in the transverse directions may be observed. The propagation properties of the spatial beams were studied near the edge of the stopband. A relation between the transmission coefficient (normalized to that at the maximum of the transmitted power without the Bragg stopband), for light at wavelengths 468 nm and 492 nm, and the input intensity is shown in Fig. 4(a). The former wavelength is located at the edge of the propagation stopband, while the latter one is located outside. The results show that, due to the blue shift of the stopband, the transmission at 468 nm increases with the input intensity. On the other hand, at 492 nm, i.e., away from the stopband, the change of the transmission is much less significant compared to the change of the transmission at 469 nm, which can be up to seven times higher. A 25% change of the transmission may be explained as resulting from the saturable absorption by the doping dye solvent, as well as from the possible variation of the Fabry-Perot interference. For a high input intensity of 1.2 MW/cm^2 , the transmission at 468 nm is approaching its value in the bulk sample, suggesting that the stopband effect is completely eliminated by the nonlinearity. In principle, the effective power-induced stopband suppression may facilitate the generation of Bragg solitons [14].

The output profile of the beam was measured at 468 nm, see Fig. 4(b). At low input intensities, the light is Bragg-reflected backward, hence the transmission beam is not observed. As the input intensity increases, the self-defocusing nonlinearity gives rise to the blue shift of the photonic stopband, which allows the input beam to propagate through the sample with strong transverse divergence. When the intensity increases further, the self-defocusing nonlinearity saturates due to the above-mentioned

absorption saturation, in which case the beam propagation features the normal linear diffraction.

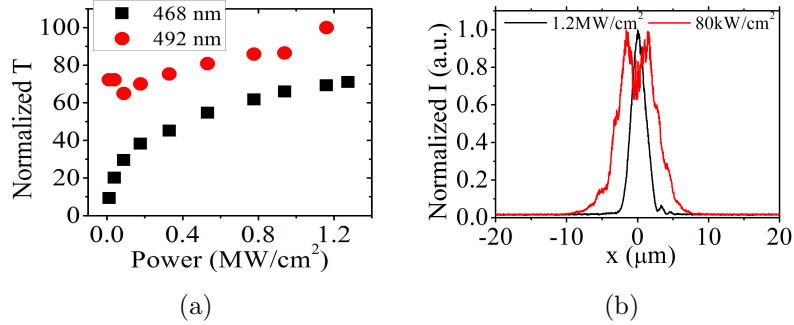


Figure 4. (Color online) (a) The relation between the transmission coefficient (normalized to the maximum of the transmitted power in the absence of the Bragg bandgap) at wavelengths 468 nm and 492 nm, and the input intensity. (b) The saturation of the expansion of the output profile at sufficiently high input intensities.

4. The theoretical model

The blue shift of the stopband indicates that the average refractive index is reduced by the high-intensity pump, which may be considered as a manifestation of the self-defocusing Kerr effect caused by the photo-induced reorientation in the CLC. The couple-mode theory has been widely used for the description of the nonlinear propagation in 1D photonic structures [1, 2, 14]. As seen in Fig. 4(a), the bandgap shift increases with the pump power, and then reaches saturation at the power exceeding $0.7 \text{ MW}/\text{cm}^2$, because of the absorption saturation by the dopant dye, as explained above. Accordingly, the couple-mode equations can be introduced with the saturation nonlinearity:

$$\pm i \frac{\partial E_{\pm}^{CP}}{\partial z} + F \frac{\partial^2 E_{\pm}^{CP}}{\partial x^2} + \delta E_{\pm}^{CP} - \gamma \frac{|E_{\pm}^{CP}|^2 + |E_{\mp}^{CP}|^2}{1 + c(|E_{\pm}^{CP}|^2 + |E_{\mp}^{CP}|^2)} E_{\pm}^{CP} + \kappa E_{\mp}^{CP} = 0, \quad (1)$$

where $|E_{\pm}^{CP}|^2$ denotes the power density of the forward and backward circular-polarized (CP) waves, z and x are the propagation distance and transverse coordinate, respectively, $\gamma = kn_2$ is the nonlinearity strength, which can be changed by the external electric field, with k being the wavenumber and n_2 the material nonlinear coefficient, c is the saturation coefficient with the same dimension as n_2 , $\kappa = \pi dn/\lambda_B$ is the effective reflectivity, where dn is the amplitude of the refractive-index modulation, and $\delta = 2\pi(n_{\text{eff}}\lambda^{-1} - \lambda_B^{-1})$ measures the detuning of the input from the Bragg wavelength, which is determined by the CLC period, and can be altered by temperature. Factor $F = 1/(2k)$ is the Fresnel diffraction strength.

To analyze the spatial-propagation dynamics of light, we performed numerical simulations of Eqs. (1) with the input wavelength located at the red edge of the stopband

with the following natural boundary conditions (b.c.):

$$E_+^{CP}(z = 0, x) = A_0 \text{sech}(x/w), \quad E_-^{CP}(z = L, x) = 0, \quad (2)$$

where A_0 represents the amplitude of input field, w is the beam's width, and L is the length of the sample. Equations (1) with b.c. (2) were solved by means of the finite-difference method. In the simulations, the coordinates and field amplitude were scaled, so as to set the span of the transverse coordinate to be $-1 < x < +1$, and the propagation distance varying in the interval of $0 < z < 5$. The coupling coefficient is fixed as $\kappa = 0.7$, and detuning $\delta = -0.65$ (which is located at the edge of the stopband). The other parameters were set as $\gamma = 1.5$, $c = 1$, $w = 0.01$, and $F = 4 \times 10^{-5}$.

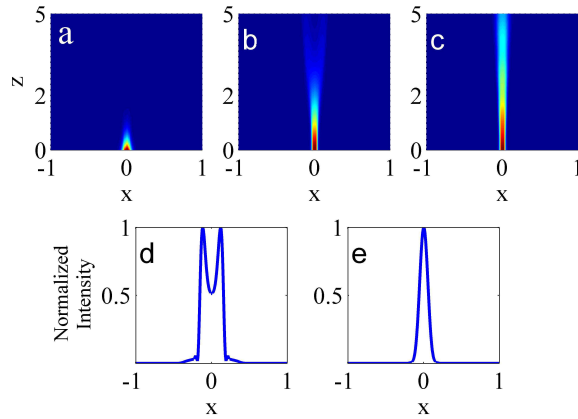


Figure 5. (Color online) Theoretical results for the propagation in the CLC, showing that, in panel (a), the low-intensity beam cannot penetrate the sample due to the reflection by the stopband. As the intensity increases, the beam penetrates the sample, featuring diffraction due to the self-defocusing nonlinearity. The respective propagation picture and the beam cross section are shown in panels (b) and (d). As the intensity increases further, the effective normal diffraction is established, see the propagation picture and the corresponding beam cross section shown in panels (c) and (e).

Typical examples of the simulated propagation are displayed in Fig. 5. At low input intensities, the input light is Bragg-reflected backward. As the input intensity increases, the self-defocusing nonlinearity gives rise to the blue shift of the stopband, which allows the input beam to propagate through the sample with strong divergence. When the intensity increases further, the divergence of the beam gets suppressed due to the saturation of the nonlinearity. Finally, the self-defocusing is totally suppressed due to the saturation, and the beam propagates effectively featuring the normal linear diffraction. Detailed comparison (shown in Fig.5(b)) demonstrates that the propagation regimes predicted by the simulations accurately match the experimental observations. The normalized intensity in Fig. 5(e) is about 15 times larger than the normalized intensity in Fig. 5(d). The width at half maximum of Fig. 5(d) is 3 times wider than Fig. 5(e). This results are well in agreement with the experimental results.

5. Conclusion

The subject of this work is the nonlinear light propagation in doped samples of CLC. By using the dye-doped CLC, the nonlinear threshold and nonlinearity length are substantially reduced, allowing one to achieve strong modulation of the intensity and spatial distribution under low input powers in a compact micro-device. The propagation of light with the wavelength located near the edge of the stopband is studied experimentally and simulated numerically. Due to the self-defocusing nonlinear effect in the CLC, the intrinsic stopband can be shifted, leading to a substantial enhancement of the transmission and strong divergence of the beam. As the input power keeps increasing, the self-defocusing-induced divergence of the beam is suppressed, due to the saturation of the nonlinearity. The system of couple-mode equations was used to model the propagation of the light beams in the CLC. Results of the simulations match the experimental observations well. The setting introduced here may find applications to the design of optical switching, power limiters, beam shapers, and optical buffering.

References

- [1] R. Slusher and B. J. Eggleton, 2003, *Nonlinear Photonic Crystals*, (Berlin, Springer-Verlag).
- [2] Y. Kivshar and G. Agrawal, 2003, *Optical Solitons: From Fibers to Photonic Crystals* (London, Academic).
- [3] B. A. Malomed, D. Mihalache, F. Wise, and L. Torner, 2005, *J. Opt. B: Quant. Semicl. Opt.* **7**, R53.
- [4] F. Lederer, G. I. Stegeman, D. N. Christodoulides, G. Assanto, M. Segev, and Y. Silberberg, 2008, *Phys. Rep.* **463**, 1.
- [5] Y. V. Kartashov, V. A. Vysloukh, and L. Torner, 2009, *Progr. Opt.* **52**, 63.
- [6] Y. V. Kartashov, B. A. Malomed, and L. Torner, 2011, *Rev. Mod. Phys.* **83**, 247.
- [7] M. Scalora, J. P. Dowling, C. M. Bowden, and M. J. Bloemer, 1994 *Phys. Rev. Lett.* **73**, 1368-1371.
- [8] S. Laroche, Y. Hibino, V. Mizrahi, and G. I. Stegeman, 1990, *Electron. Lett.* **26**, 1459-1460.
- [9] N. D. Sankey, D. F. Prelewitz, and T. G. Brown, 1992, *Appl. Phys. Lett.* **60**, 1427-1429.
- [10] P. Millar, R. M. De La Rue, T. F. Krauss, J. S. Aitchison, N. G. R. Broderick, and D. J. Richardson, 1999, *Opt. Lett.* **24**, 685-687.
- [11] H. G. Winful, J. H. Marburger, and E. Garmire, 1979, *Appl. Phys. Lett.* **35**, 379.
- [12] A. V. Andreev, A. V. Balakin, I. A. Ozheredov, A. P. Shkurinov, P. Masselin, G. Mouret, D. Boucher, 2001, *Phys. Rev. E.* **63**, 016602.
- [13] F. Schreier and O. Bryngdahl, 2000, *Opt. Commun.* **185**, 227.
- [14] C. M. de Sterke, and J. E. Sipe, 1994, *Progr. Opt.* **33**, 205.
- [15] B. J. Eggleton, R. E. Slusher, C. M. de Sterke, P. A. Krug and J. E. Sipe, 1996, *Phys. Rev. Lett.* **76**, 1627.
- [16] J. T. Mok, C. M. de Sterke, I. C. M. Littler, and B. J. Eggleton, 2006, *Nature Phys.* **2**, 775.
- [17] J. Y. Zhou, H. G. Shao, J. Zhao, and K. S. Wong, 2005, *Opt. Lett.* **30**, 1560-1562.
- [18] S. Fu, Y. Liu, Y. Li, L. Song, J. Li, B. A. Malomed, and J. Zhou, 2013, *Opt. Lett.* **23**, 5047-5050.
- [19] J. P. Prineas, J. Y. Zhou, J. Kuhl, H. M. Gibbs, G. Khitrova, S. W. Koch, and A. Knorr, 2002, *Appl. Phys. Lett.* **81**, 4332-4334.
- [20] D. Mandelik, R. Morandotti, J. S. Aitchison, and Y. Silberberg, 2004, *Phys. Rev. Lett.* **92**, 093904.
- [21] J. Feng, 1993, *Opt. Lett.* **18**, 1302-1304.
- [22] R. F. Nabiev, P. Yeh, and D. Botez, 1993, *Opt. Lett.* **18**, 1612-1614.

- [23] J. Schöllmann, R. Scheibenzuber, A. S. Kovalev, and A. P. Mayer, 1999, Phys. Rev. E. **59**, 4618-4629.
- [24] J. Atai and B. A. Malomed, 2001, Phys. Lett. A. **284**, 247-252.
- [25] A. A. Sukhorukov and Y. S. Kivshar, 2002, J. Opt. Soc. Am. B. **19**, 772-781.
- [26] B. A. Malomed, T. Mayteevarunyoo, E. A. Ostrovskaya, and Y. S. Kivshar, 2005, Phys. Rev. E. **71**, 056616.
- [27] A. Ciattoni, C. Rizza, E. DelRe, and E. Palange, 2007, Phys. Rev. Lett. **98**, 043901.
- [28] N. Tamaoki, 2001, Advanced Materials. **13**, 1135.
- [29] I. Janossy, 1994, Phys. Rev. E. **49**, 2957.
- [30] T. V. Truong, L. Xu, and Y. R. Shen, 2005, Phys. Rev. E. **72**, 051709.
- [31] L. Narducci, 2002, Liquid Crystals today, **11**, 101002.
- [32] M. Li, P.-Q. Zhang, J. Guo, X.-S. Xie, Y.-K. Liu, B. Liang, J.-Y. Zhou, and Y. Xiang, 2008, Chinese Phys. Lett. **25**, 108.
- [33] X. Ying, M. Li, L. Tao, L. Jie, and J. Y. Zhou, 2007, Appl. Phys. A: Materials Science & Processing. **86**, 207 (2007).
- [34] Y. Xiang, T. Li, and J. Lin, 2006, Physics Letters A. **357**, 159.
- [35] H.-C. Yeh, 2011, Opt. Express. **19**, 5500.
- [36] J. Hwang, N. Y. Ha, H. J. Chang, B. Park, and J. W. Wu, 2004, Opt. Lett. **29**, 2644-2646.
- [37] Tatsunosuke Matsui and Masahiro Kitaguchi, 2010, Appl. Phys. Express, **3**, 061701.
- [38] V. A. Belyakov, V. E. Dmitrienko and V. P. Orlov, 1979, Sov. Phys. Usp. **22** 64
doi:10.1070/PU1979v022n02ABEH005417
- [39] G. S. Chilaya, 2006, Crystallogr. Rep. **51**, S108.
- [40] F. A. Sala and M. A. Karpierz, 2012, Mol. Cryst. Liq. Cryst. **558**, 176.
- [41] A. Fratalocchi et al., Opt. Express **13**, 1808 (2005)
- [42] D. Wei et al., Two-wave mixing in chiral dye-doped nematic liquid crystals Optics Letters **37**, 734, (2012).
- [43] D. Wei, U. Bortolozzo, J. P. Huignard, and S. Residori, Slow and stored light by photoisomerization induced transparency in dye doped chiral nematics, Opt. Express, **21**, 19544 (2013)
- [44] Liyan Song, Shenhe Fu, Yikun Liu, Jianying Zhou, Vladimir G. Chigrinov, and Iam Choon Khoo, 2013, Opt. Lett, **38**, 5040.
- [45] I. C. Khoo, Hong Li, Yu Liang, 1993, IEEE JOURNAL OF QUANTUM ELECTRONICS, **29**, 1444.
- [46] I.C.Khoo, 1995, "Liquid Crystals: Physical Properties and Nonlinear Optical Phenomena", (New York, Wiley).
- [47] P. Klysubun and G. Indebetouw, 2002, "Transient and steady state photorefractive responses in dye-doped nematic liquid crystal cells," J. Appl. Phys. **91**, 897.

Acknowledgments

The author thanks Professor I. Janossy for the useful discussions. This project is supported by National Basic Research Program of China (2012CB921904), and by the Chinese National Natural Science Foundation (11074054). The work of Y. Li was supported by the German-Israel Foundation through grant No. I-1024-2.7/2009, and by a postdoctoral fellowship from the Tel Aviv University.